

Date of Issue: May 14, 1984

K/PS--5042

DE86 006341

SAMPLING, CHARACTERIZATION, AND REMOTE SENSING OF AEROSOLS
FORMED IN THE ATMOSPHERIC HYDROLYSIS OF URANIUM HEXAFLUORIDE

W. D. Bostick
W. H. McCulla
P. W. Pickrell

Materials and Chemistry Technology Department
Process Support Division

Martin Marietta Energy Systems, Inc.
Oak Ridge Gaseous Diffusion Plant
Oak Ridge, Tennessee

Prepared for the U.S. Department of Energy
Under Contract No. DE-AC05-84OR21400

DISCLAIMER

This report was prepared as an account of work sponsored by an agency of the United States Government. Neither the United States Government nor any agency Thereof, nor any of their employees, makes any warranty, express or implied, or assumes any legal liability or responsibility for the accuracy, completeness, or usefulness of any information, apparatus, product, or process disclosed, or represents that its use would not infringe privately owned rights. Reference herein to any specific commercial product, process, or service by trade name, trademark, manufacturer, or otherwise does not necessarily constitute or imply its endorsement, recommendation, or favoring by the United States Government or any agency thereof. The views and opinions of authors expressed herein do not necessarily state or reflect those of the United States Government or any agency thereof.

DISCLAIMER

Portions of this document may be illegible in electronic image products. Images are produced from the best available original document.

TABLE OF CONTENTS

	<u>Page</u>
SUMMARY.....	5
INTRODUCTION.....	5
COMPOSITION OF HYDROLYSIS PRODUCTS.....	5
PHYSICAL CHARACTERIZATION OF AEROSOL COMPONENTS.....	6
STATIONARY AEROSOL SAMPLING DEVICES.....	16
REMOTE SENSING OF AEROSOL CONSTITUENTS.....	23
CONCLUSION.....	32
REFERENCES.....	34

SUMMARY

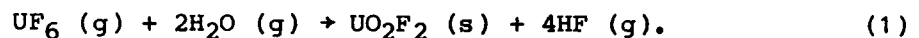
When gaseous uranium hexafluoride (UF_6) is released into the atmosphere, it rapidly reacts with ambient moisture to form an aerosol of uranyl fluoride (UO_2F_2) and hydrogen fluoride (HF). As part of our Safety Analysis program, we have performed several experimental releases of UF_6 in contained volumes in order to investigate techniques for sampling and characterizing the aerosol materials. The aggregate particle morphology and size distribution have been found to be dependent upon several conditions, including the temperature of the UF_6 at the time of its release, the relative humidity of the air into which it is released, and the elapsed time after the release. Aerosol composition and settling rate have been investigated using stationary samplers for the separate collection of UO_2F_2 and HF and via laser spectroscopic remote sensing (Mie scatter and infrared spectroscopy).

INTRODUCTION

Uranium hexafluoride is handled in very large quantities, at pressures which may be either above or below atmospheric conditions, in both the gaseous diffusion and gas centrifuge uranium enrichment processes. There is, thus, the potential for an accidental release of significant amounts of UF_6 to the environment with the possible exposure of plant personnel and the surrounding population to various uranium and fluoride species. The Department of Energy (DOE) has mandated a safety analysis effort to evaluate the potential for accident and to predict the human health consequences of any postulated UF_6 release. In order to make these predictions, it is necessary to (1) understand which toxic materials are involved and those characteristics which may affect the dispersion of the material, (2) be able to predict the concentration level and exposure duration for each toxic material, and (3) estimate the human health consequences from such an exposure. This communication summarizes some of our recent investigations on the atmospheric hydrolysis of UF_6 and the characterization of the aerosols formed under controlled conditions within an enclosed volume. Emphasis has been placed upon product identification and upon the determination of those properties which affect the dispersion and detection of the products. Work on effective sampling techniques and instrumental approaches for the remote sensing of aerosol constituents is also described.

COMPOSITION OF HYDROLYSIS PRODUCTS

When it is released into the atmosphere, gaseous UF_6 is rapidly hydrolyzed by ambient moisture to form UO_2F_2 and HF:



"Anhydrous" UO_2F_2 is hygroscopic,¹ as is HF;² hence, both species tend to become hydrated. The particulate UO_2F_2 is readily visible as a white aerosol cloud or "smoke," which may rise and be dispersed into the environment.

Fallout materials from the experimental release of UF_6 within an enclosed volume have been collected and examined by x-ray diffraction (XRD).³ In general, these materials appear to be of variable composition, which seldom exactly match reference standards (cf. Table 1). On occasion, however, stable hydrates or HF hydrates of UO_2F_2 have been identified in the fallout material.³

The nature of a possible association between the UO_2F_2 and HF components of the aerosol is not yet satisfactorily established. Possible mechanisms for such an association (if it occurs) may include gas-phase sorption of hydrated HF onto UO_2F_2 , or the cosedimentation of both species as fallout material. Chemical examination of the fallout material (Fig. 1) confirms the presence of an excess of fluoride (i.e., a molar ratio $\text{F}/\text{U} > 2$) in the initial fallout material; this excess fluoride is lost over a period of time, possibly due to the evaporation of HF or the ligand exchange between sorbed HF and atmospheric moisture. After approximately 2 days' equilibration with the atmosphere, the empirical formula for the fallout material becomes $\text{UO}_2\text{F}_2 \cdot n\text{H}_2\text{O}$, where n represents a variable degree of hydration. This UO_2F_2 hydrate demonstrates little or no affinity to sorb anhydrous HF vapor.

PHYSICAL CHARACTERIZATION OF AEROSOL COMPONENTS

Some physical characteristics of the UF_6 -release fallout material are summarized in Table 2. The refractive index of the particulates is important in the detection of these materials with the use of light-scattering techniques. The particle density is an important parameter in determining the sedimentation rate for the airborne particulates. Tsvetkov et al⁴ report that the particle density of UO_2F_2 is strongly affected by the degree of hydration; Figure 2 reproduces some of their data. If one compares the measured density of UF_6 -release fallout material (Table 2) to the data presented in Figure 2, there is the suggestion that the fallout material may contain an average of two to three waters of hydration per uranyl molecule.

The geometric particle size is an important determinant in the detection of particulates by light-scatter techniques and in the collection of these materials with use of filtration sampling devices (q.v.). Lux⁵ has used the technique of electron microscopy to examine fallout material formed in the experimental release of UF_6 within an experimental chamber under a variety of atmospheric conditions. He concludes that relative humidity (20% to 90% R.H.), ambient air temperature (0-40°C); and sample size do not seriously affect the UO_2F_2 particulate size distribution (0.5 to 3.0 μm). Experimental releases were effected under static, dynamic, and simulated catastrophic conditions. Under

Table 1. Preparation and properties of some solid-phase uranyl fluoride reference materials

Material designation	Synthesis	Reference/Comments
"Anhydrous" uranyl fluoride	$\text{UO}_3 + \text{HF};$ Uranyl acetate + HF; $\text{UF}_6 + \text{H}_2\text{O}$	Various syntheses yield products with virtually indistinguishable x-ray diffraction (XRD) patterns ^{1,2} . Material is highly hygroscopic. Thermal decomposition occurs at $> 300^\circ\text{C}$.
"Uranyl Fluoride II" (hydrate)	"Anhydrous" UO_2F_2 exposed to atmospheric moisture for a few days	Our preparation according to the procedure of Narasimham ³ gave material with the probable composition $\text{UO}_2\text{F}_2 \cdot 1.5\text{H}_2\text{O}$, as identified by XRD.
Uranyl fluoride hydrates	$\text{UO}_2\text{F}_2 + \text{H}_2\text{O}$ (sealed ampoule, 120°C) $\rightarrow \text{UO}_2\text{F}_2 \cdot n\text{H}_2\text{O}$ ($n=1-4$)	XRD patterns recorded by Seleznev et al. ⁴ Crystals or solid solutions obtained, dependent upon stoichiometry. ^{4,5} Pycnometric measurements of density decreases with increasing hydration. ⁵
"Basic salts" of uranyl fluoride	$\text{UO}_3 + \text{H}_2\text{O} + \text{HF} \rightarrow \text{UO}_2(\text{OH})_x\text{F}_{2-x} \cdot y\text{H}_2\text{O}$ ($x=0.3-1.2$, $y=1,2$)	XRD patterns recorded by Seleznev et al. ⁶
"Hydrogen fluoride adducts" of uranyl fluoride	$\text{UO}_3 + \text{HF}$ (excess) $\rightarrow \text{UO}_2\text{F}_2 \cdot x\text{HF} \cdot y\text{H}_2\text{O}$	Compounds of variable composition. XRD patterns recorded by Seleznev et al. ⁷

¹W. H. Zachariassen, *Acta Cryst.*, **1**, 277 (1948).

²L.H. Brooks, E. V. Garner, and E. Whitehead, "Chemical and X-ray Crystallographic Studies on Uranyl Fluorides," IGR-RN/CA-277 (1956).

³K.V. Narasimham, "Absorption Spectra of Uranyl Halides," in J. R. Ferraro and J. S. Ziomek (eds), *Developments in Applied Spectroscopy*, Vol. 2, Plenum Press (1963), pp. 142-159.

⁴V. P. Seleznev, A. A. Tsvetkov, B. N. Sudarikov, and B. V. Gromov, *Russ. J. Inorg. Chem.*, **17**, 1356 (1972).

⁵A. A. Tsvetkov, V. P. Seleznev, B. N. Sudarikov, and B. V. Gromov, *Russ. J. Inorg. Chem.*, **17**, 1048 (1972).

⁶V. P. Seleznev, A. A. Tsvetkov, B. N. Sudarikov, B. V. Gromov, and Y. M. Khozhainov, *Russ. J. Inorg. Chem.*, **17**, 1644 (1972).

⁷V. P. Seleznev, A. A. Tsvetkov, and Y. M. Khozhainov, *Russ. J. Inorg. Chem.*, **16**, 1530 (1971).

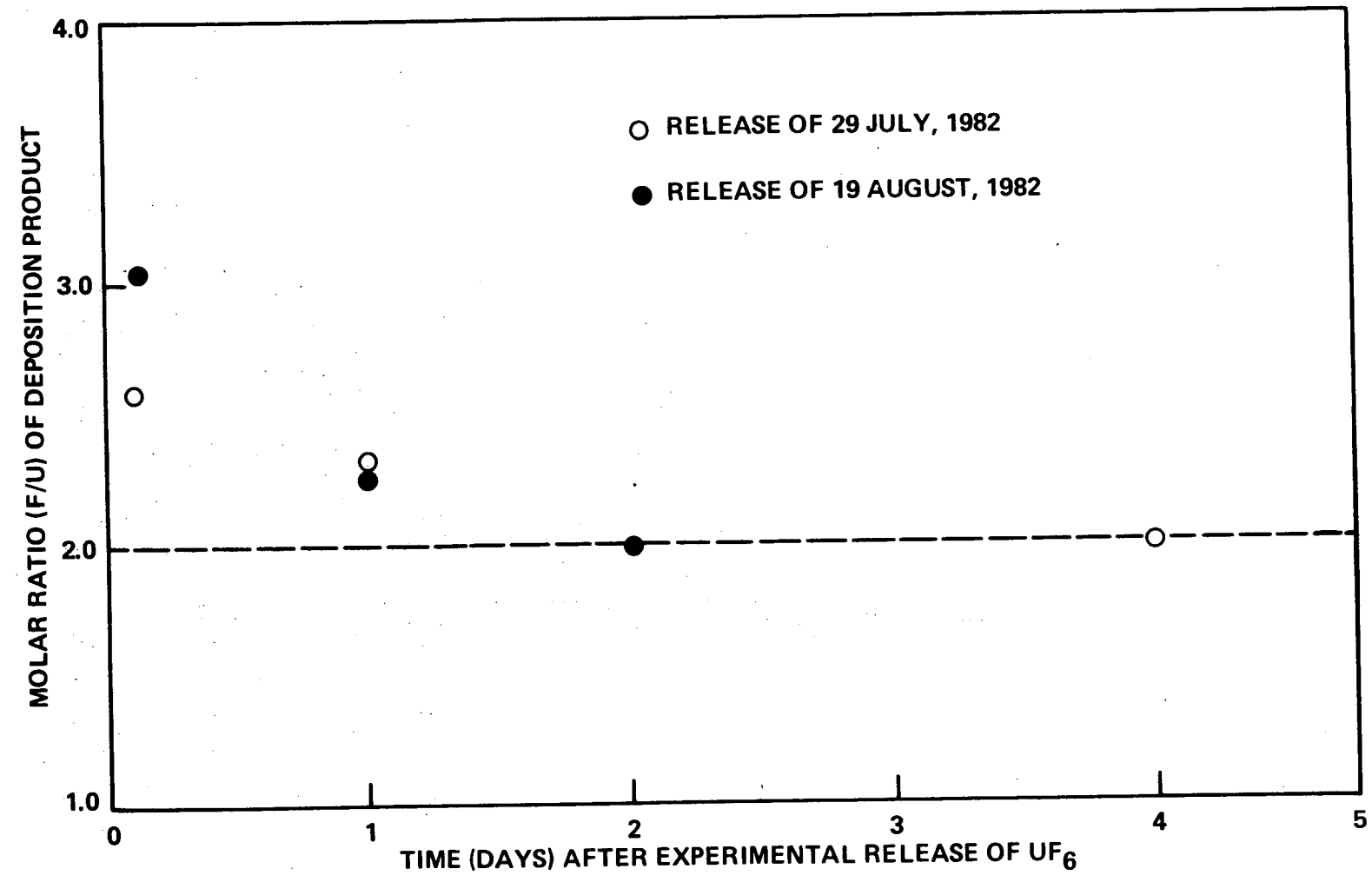


Figure 1. Ligand exchange between HF and H₂O on the fallout material from the atmospheric hydrolysis of UF₆.

Table 2. Selected physical characteristics of typical uranyl fluoride particulates from the atmospheric hydrolysis of uranium hexafluoride

Particle size (geometric)	
median	~ 0.6-1.2 μm^*
range	~ 0.3-3.0 μm^*
	~ 1-5 μm^{**}
Density (pyknometric)	~ 4.13 g/cm^3
Refractive index (white light)	~ 1.54***

*Electron microscopy data reported by C. J. Lux.⁵

**Coulter counter data reported by H. Conley and M. G. Otey, KY-725, Rev. 1, UO₂F₂ Particle Size Analysis, Paducah Gaseous Diffusion Plant, Paducah, Kentucky, July 1983.

***Determined by central illumination method [W. C. McCrone and J. G. Dally, The Particle Atlas (2nd ed.), Volume I: Principles and Techniques, Ann Arbor Science (1973), p. 74]

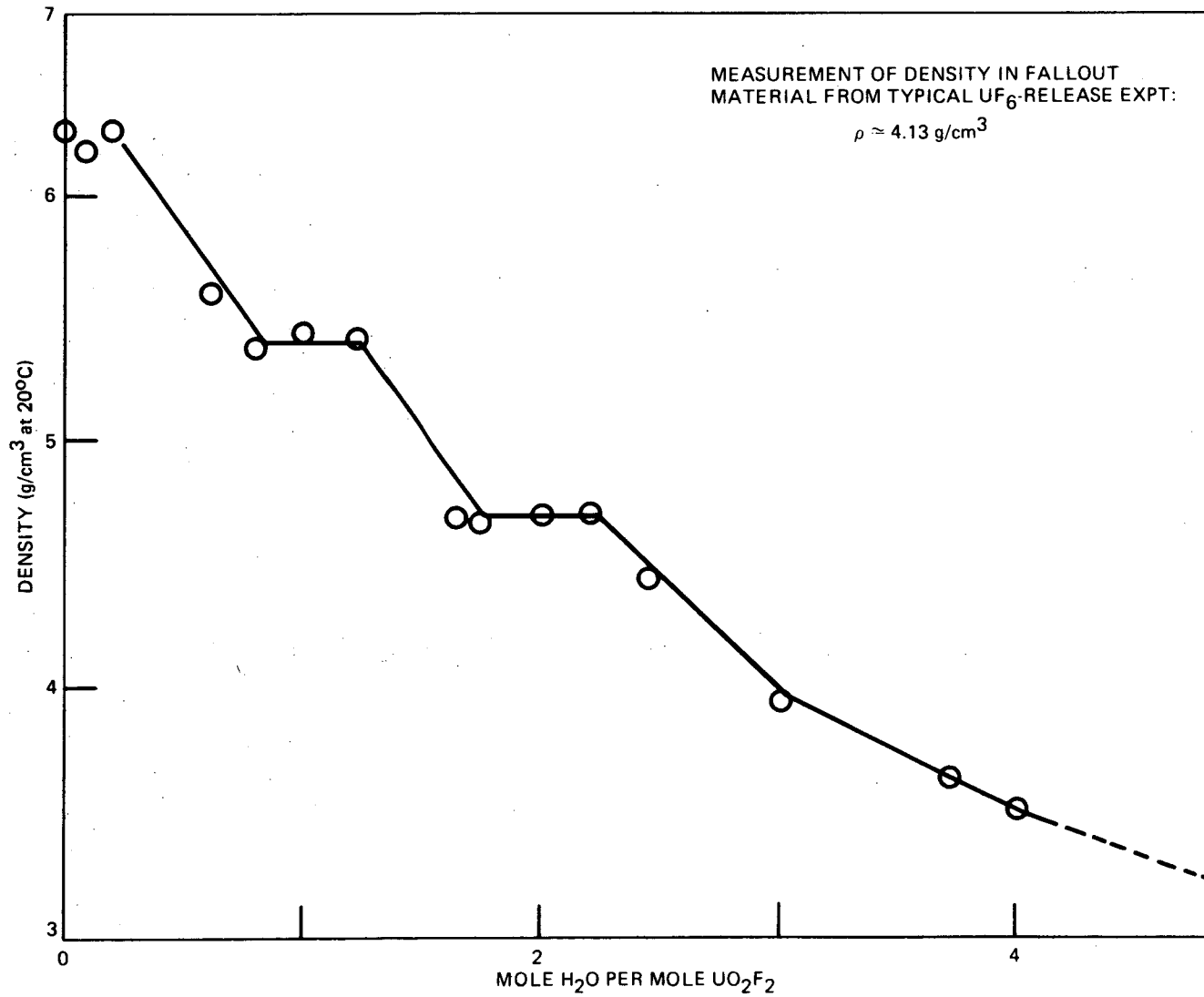


Figure 2. Dependence of density upon composition in the UO₂F₂-H₂O system. Data from Reference 4.

static conditions, UF_6 is released into stagnant air. Dynamic conditions refer to the release into a simulated cross-wind of 2 to 4.5 mph. Catastrophic conditions were simulated by the rapid release and evaporation of liquid UF_6 . The mode of release does appear to affect the particle size distribution (Fig. 3); this may be a consequence of the initial rate of dispersion and the subsequent effect upon particle agglomeration.

Pickrell³ has also applied electron microscopy to the examination of materials formed in the atmospheric hydrolysis of UF_6 . Somewhat in contrast to the findings of Lux, he reports that particle agglomeration and morphology are dependent upon several factors, including the temperature of the UF_6 at the time of its release, the relative humidity of the ambient air into which the UF_6 is released, and the time which had elapsed since the instant of release.

The temperature of the UF_6 at the time of its release appears to affect both the initial rate of dispersion (hence, the rate of particle agglomeration) and the fraction of material which actually becomes airborne. If the initial temperature of the UF_6 is only slightly above its sublimation point ($\sim 56^\circ C$), released material may be cooled upon expansion and condense. This condensate may sediment rapidly to the bottom of the test chamber and be hydrolyzed there, with a marked decrease in the airborne fraction of the total U(VI).

Figure 4 illustrates a typical particle morphology for material formed in air with relative humidity in the range of $\sim 20\%$ to 70% . These materials tend to be chain-like agglomerates comprised of individual 0.1 to $0.2 \mu m$ spheroids. In time, these agglomerates may reach 5 to $10 \mu m$ in greatest dimension, although most are considerably smaller. Due to the hygroscopic nature of UO_2F_2 , materials formed in high-humidity environments (e.g., $> 85\%$ R.H.) tend to form solutions and, therefore, become spheroidized (see Fig. 5).

The aerodynamic particle size (d_p) is the dominant factor in determining the sedimentation rate (v) of the aerosol, as predicted by the Stokes-Cunningham equation:⁶

$$v = \rho g d_p^2 (1 + 2A\lambda/d_p) / 18\eta \quad (2)$$

where ρ is the particle density, g is the gravitational acceleration, A is a numerical factor (with the approximate value of 0.9 for particles in the size range of interest), λ is the mean free path of the particle in air ($\sim 0.065 \mu m$), and η is the viscosity of air.

The aerodynamic particle size (i.e., the diameter of the sphere which mimics the aerodynamic behavior of a particle) can be measured with the use of a cascade impactor. Pickrell³ has used this technique to investigate particle size as a function of time under a variety of experimental release conditions. These data support the qualitative conclusions stated previously. In addition, preliminary statistical evaluation⁷ of some of this data has been performed. Figure 6 represents the computed distribution diagram for aerosol mass as a function

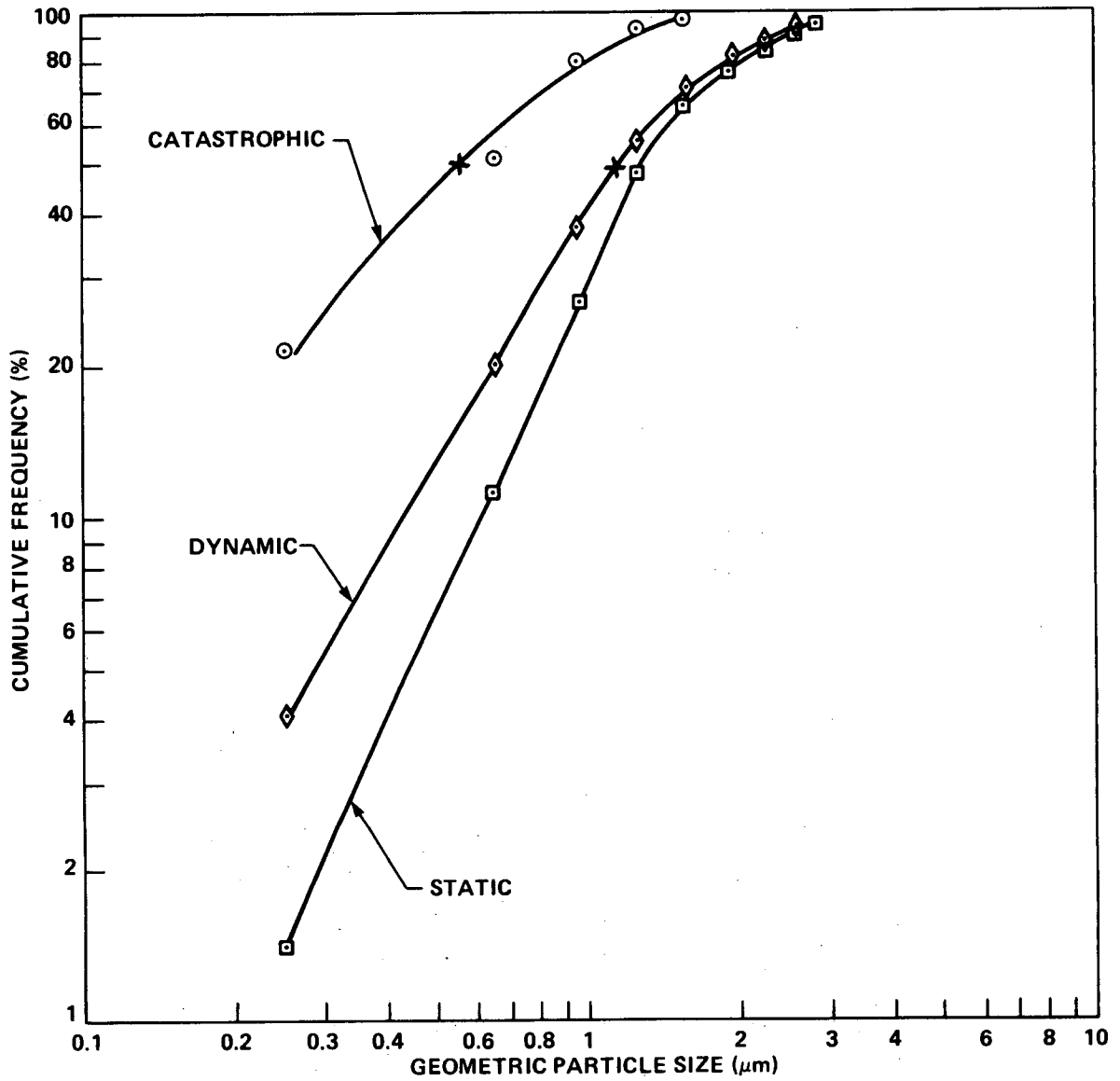


Figure 3. Geometric particle size distribution of fallout material as a function of the mode of UF_6 -release (see text). Data from Reference 5.

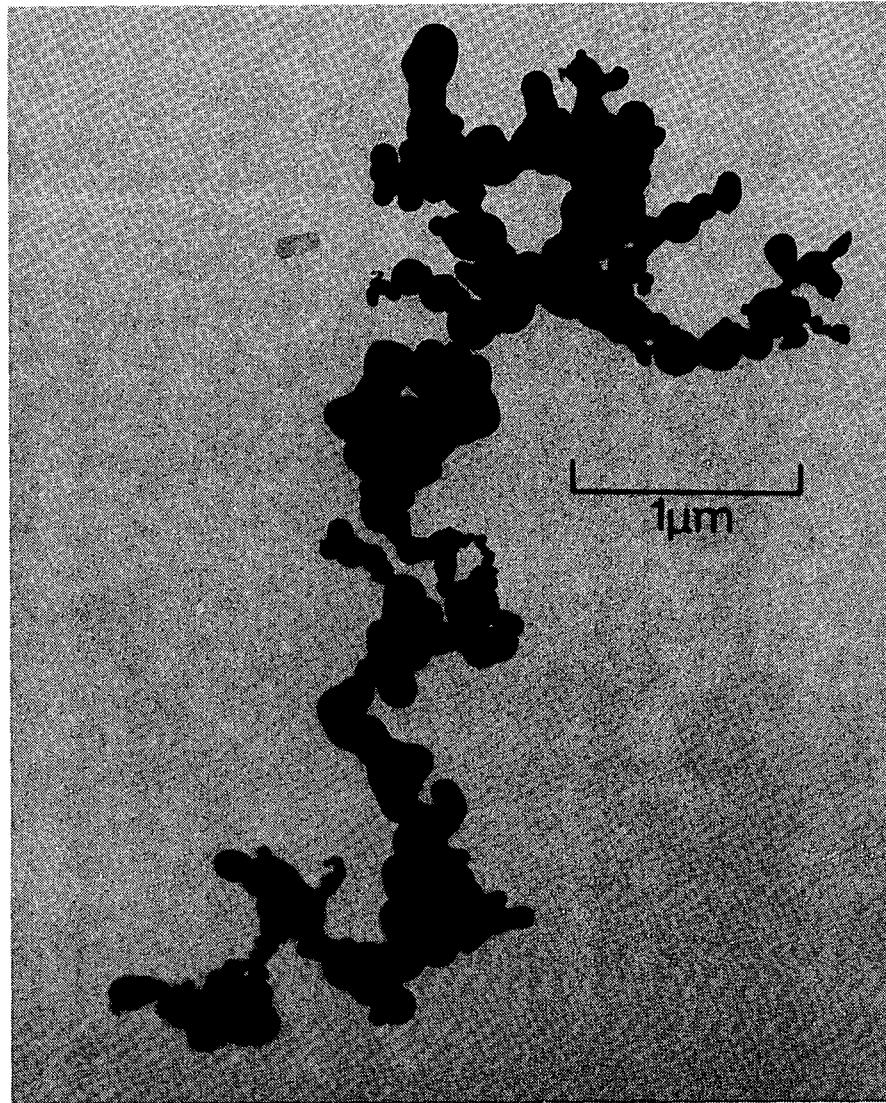


Figure 4. Electron micrograph of particulate matter collected at an interval of 2 hr following the experimental release of UF_6 into an environment with relative humidity of 45%.

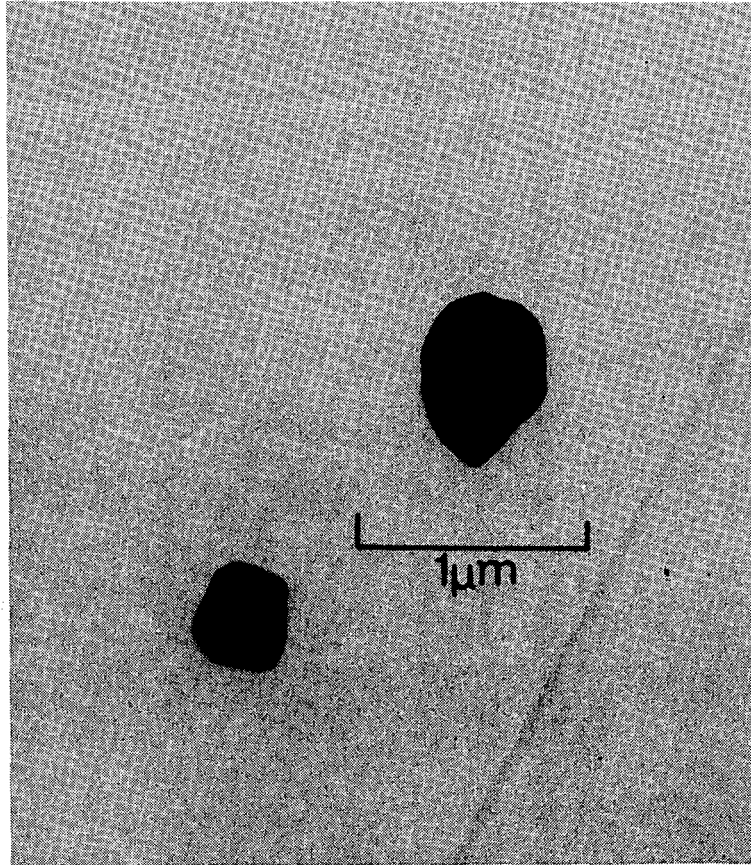


Figure 5. Electron micrograph of particulate matter formed in an environment with relative humidity of 100%.

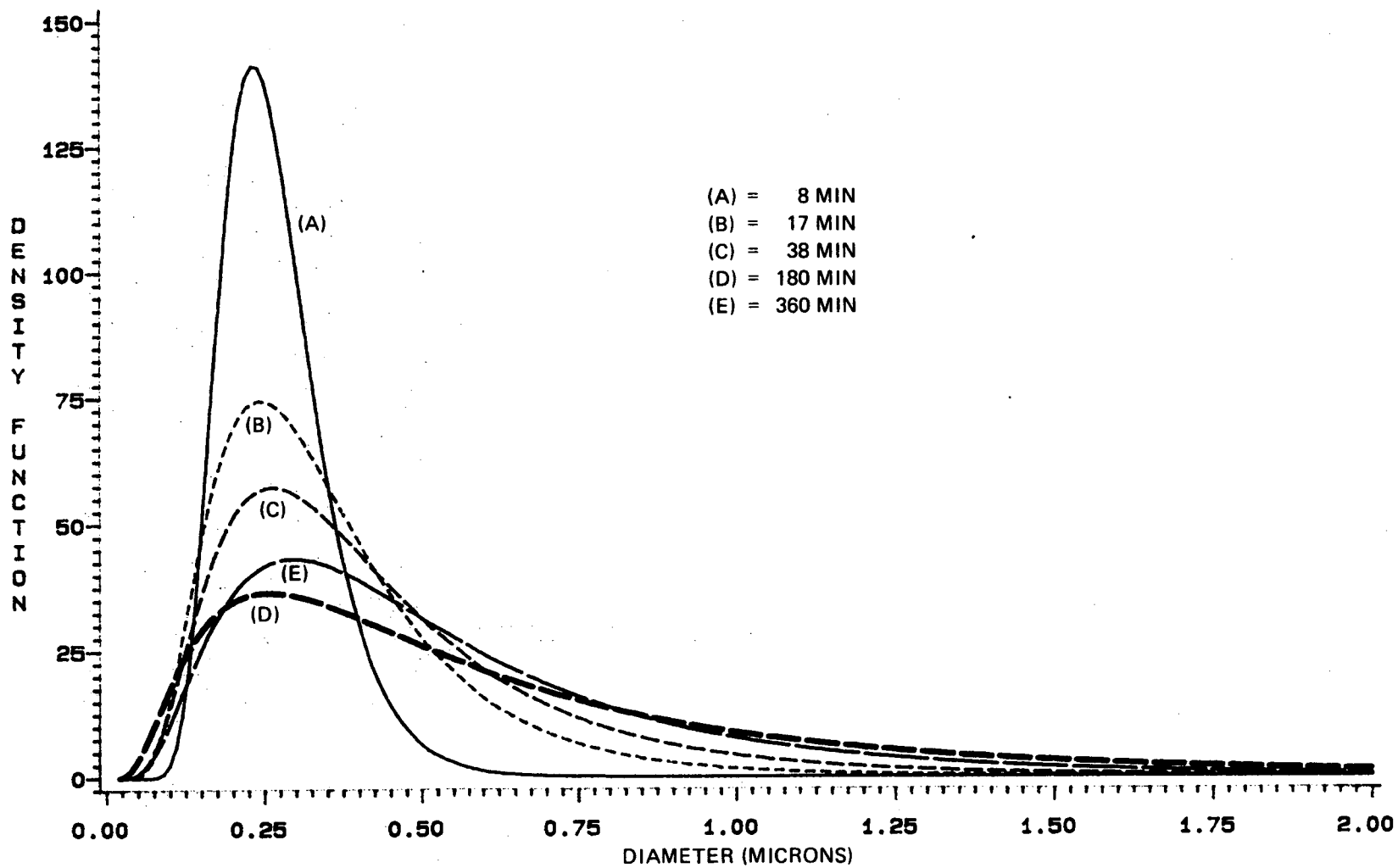


Figure 6. Computed aerosol mass distribution diagrams for aerodynamic particle size as a function of time elapsed from the release of UF_6 into an environment with relative humidity of 35%. Data from Table I of Reference 3.

of d_p for data obtained following an experimental UF_6 release. Aerodynamically, the aerosol materials behave as though they were very small particles. An initial increase in median particle size following a release of UF_6 , due to particle agglomeration, has normally been observed. At longer time, median particle size decreases due to the sedimentation of larger particles. The data shown in Figure 7 are consistent with these observations. (Note: The data presented in Figs. 6 and 7 were computed from the data of Table 1 in reference 3.)

STATIONARY AEROSOL SAMPLING DEVICES

Stationary samplers are extensively used in aerosol measurements for health physics and in dispersion modeling, due to their relative simplicity and low cost. Samples may be collected in stable, concentrated forms amenable to specific physical or chemical examination.

Dependent upon the mode of collection, stationary samplers may be used to provide either a continuous or a time-integrated response to the constituents of interest. In the continuous measurement mode, these devices may be used to provide an alarm signal for the accidental release of aerosol material. Ishida and coworkers⁸ evaluated the performance of the following systems for the detection of UF_6 -hydrolysis aerosols: an ionized smoke detector (nonspecific response to particulates), an alpha dust monitor (selective for isotopically enriched uranium), and an electrochemical sensor (fluoride ion-selective electrode). The potentiometric detection of fluoride ion (from the dissolution of UO_2F_2 and HF) was judged superior on the bases of sensitivity, selectivity, and rapid response time.

Acidic HF vapor may be collected essentially quantitatively by impinging the gas sample into a caustic scrub solution, from which it may be subsequently measured with the use of colorimetric or potentiometric analysis.^{9,10} Alternately, HF can be sorbed onto chemically treated membrane filters.^{8,10-13} The latter collection mode is especially convenient, requiring minimal apparatus or reagent, and, thus, it may be incorporated into compact and rugged field sampling units.

If particulates, such as UO_2F_2 , are to be collected separately from gaseous components, a small-pore prefilter is used. Uranyl fluoride entrapped on the prefilter may be extracted and quantitated by selective wet chemical procedures. Fluorometric analysis is the most sensitive procedure, with detectability of uranium in nanogram quantities.^{14,15}

In order to evaluate the collection efficiency of a dual membrane filter assembly for the separate collection of particulate and gaseous fluorides, it was necessary to expose the membranes to a known concentration of dilute HF vapor. This was achieved with the use of a permeation tube apparatus (Fig. 8) similar to the system used by Elfers and Decker.¹² Anhydrous HF permeates through the PTFE Teflon tube at a rate which is dependent upon the dimensions of the tube and the temperature at which it is maintained;^{12,16} the rate of permeation may be calibrated

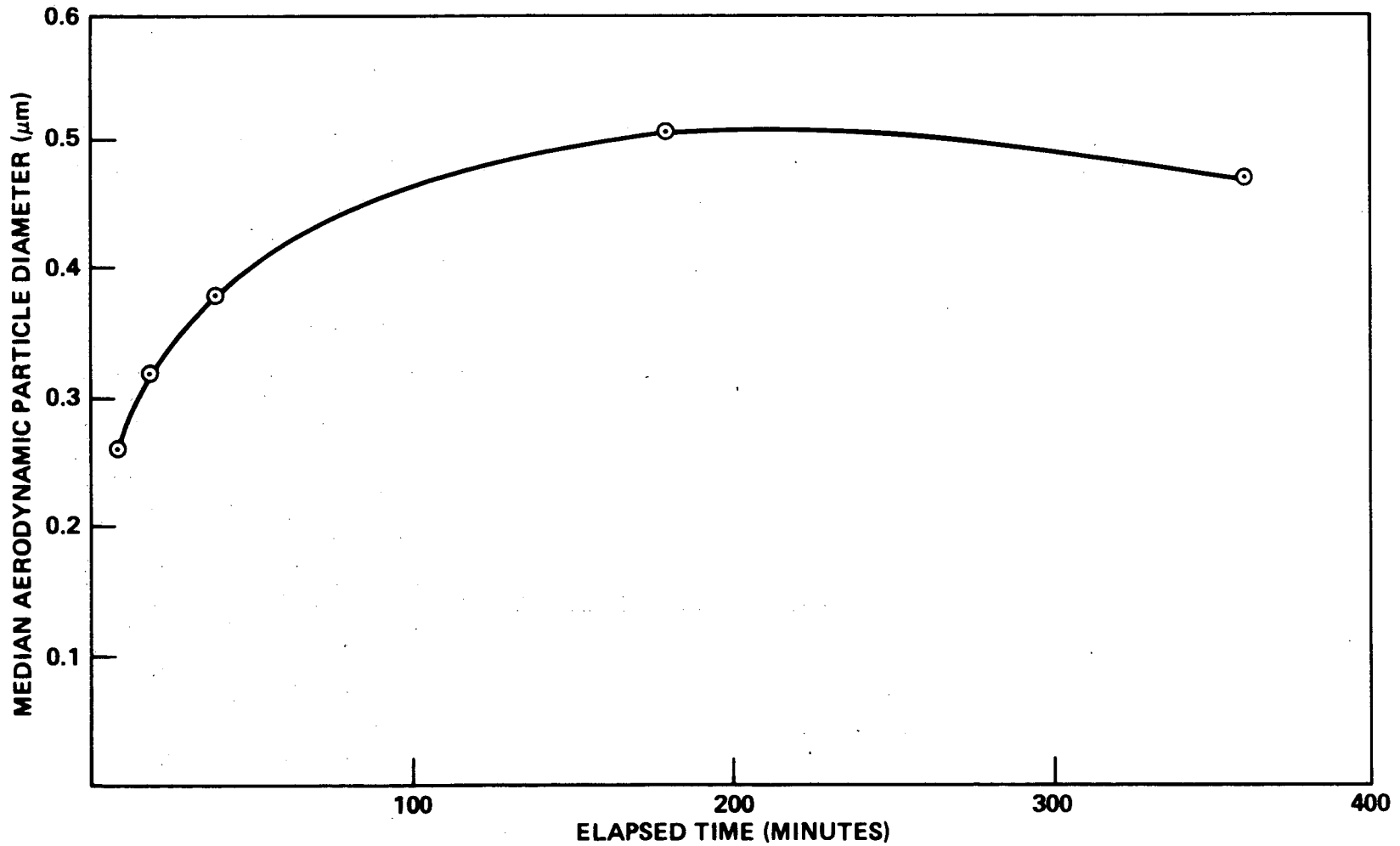


Figure 7. Estimated median aerodynamic particle size as a function of time elapsed from the experimental release of UF_6 .
Data from Table I of Reference 3.

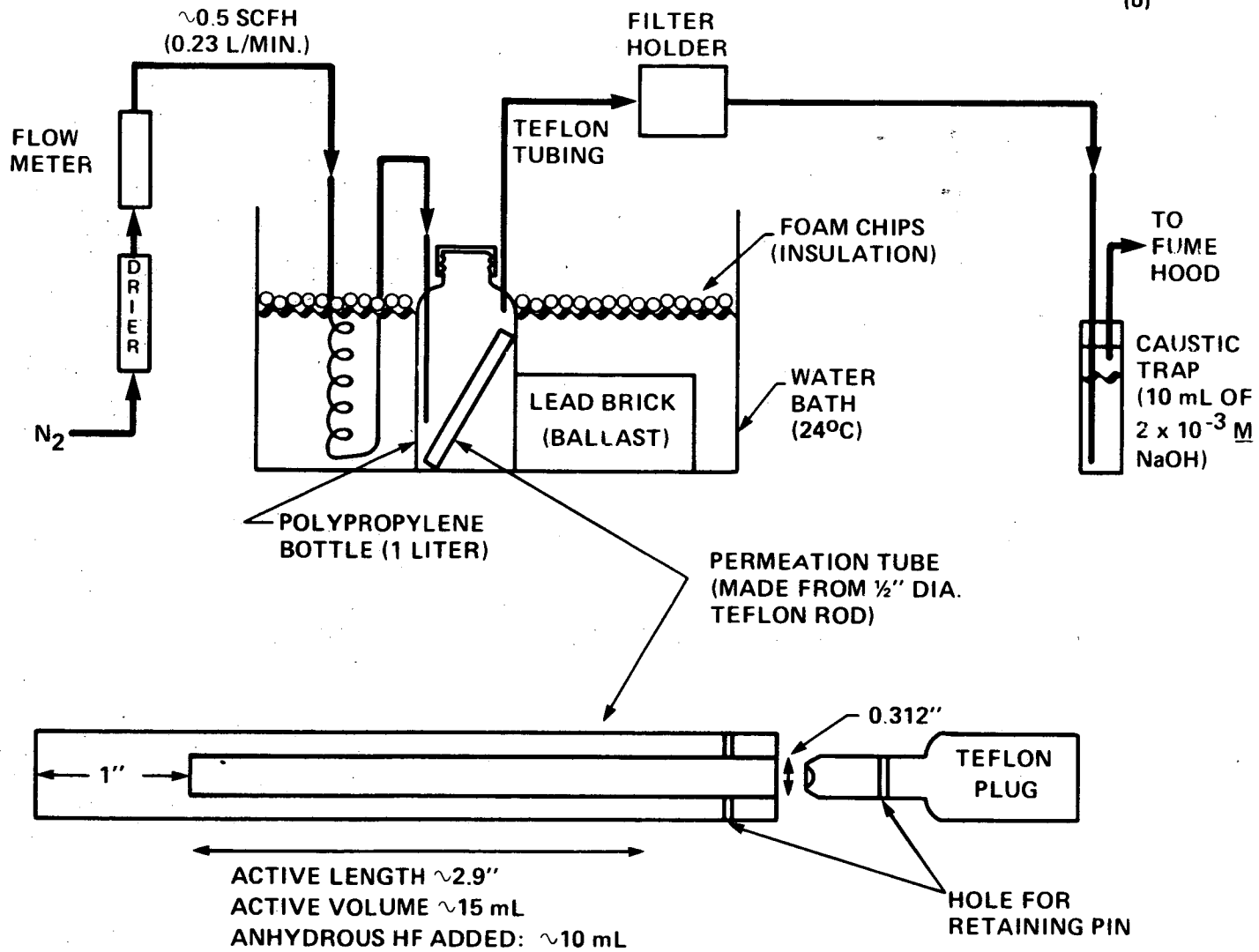


Figure 8. Construction of HF permeation tube and metering apparatus.

gravimetrically with an overall absolute accuracy of 1% to 2%,¹⁶ as demonstrated in Figure 9.

Membranes were mounted in an inexpensive, commercially available polypropylene holder (Swinnex-type, 47-mm diam, Millipore Corporation; compare this to the custom-fabricated Teflon or gold-plated holders specified in reference 14). The membranes were exposed to a flow of dilute HF vapor (~ 7 ppm), after which the retained HF was quantitatively measured. A caustic trap mounted behind the filter assembly (Fig. 8) collected any unretained HF, permitting an accurate fluoride mass balance (see Table 3).

Cellulose ester membranes impregnated with either formate¹² or carbonate¹³ are essentially quantitative in the chemisorption of HF vapor. Untreated hydrophilic cellulose ester membranes have been used as prefilters for the collection of particulate fluorides (see references 13 and 14); however, as shown by experiment 1 in Table 3, these materials are reactive with HF vapor and may lead to an erroneous mass balance for HF as collected on the treated membrane. Elfers and Decker¹² similarly report a retention of HF (up to 30%) on untreated cellulose ester membranes. In contrast, hydrophobic Teflon membranes show virtually no retention of HF, and, thus, are preferred for an accurate discrimination between particulate and gaseous fluorides. Due to the irregular structure within the membrane, a nominal 1- μm pore prefilter is highly effective in collecting submicron particles at moderate flow velocities, and, thus, should result in near-quantitative recovery of airborne UO_2F_2 particles (cf. Fig. 3).

Filter assemblies, comprised of stacked Teflon and formate-impregnated membranes, were combined with a portable, programmable, remote-controlled air sampler system¹⁷ and used to collect samples for chemical analysis following an experimental release of UF_6 (~ 1 g) into a contained volume ($\sim 0.2\text{m}^3$). The results of these analyses (colorimetric assay of U(VI), potentiometric assay of F^-) are shown in Figure 10.

Note in Figure 10 that there appears to be an exponential decrease in the mass (or molar) concentration of both the U(VI) and hydrated HF components from the gas phase as a function of time. This type of behavior is frequently observed in aerosols (e.g., reference 6, pp. 155-6), and is attributed to particle coagulation and sedimentation. Empirically, the data may be described by an expression of the form:

$$(C/C_0) = \exp(-kt) \quad (3)$$

where C is the instantaneous mass concentration of the aerosol component of interest, C_0 is the concentration at an initial time, t is the elapsed time, and k is the "mass loss constant." For the data of Figure 10, k is estimated as $\sim 0.0162 \text{ min}^{-1}$ for HF and $\sim 0.0283 \text{ min}^{-1}$ for U(VI) (i.e., the U(VI) component settles nearly twice as rapidly). In the present example, the "half-life" for airborne material is ~ 43 min for HF and ~ 25 min for U(VI). For experiments conducted within an enclosed volume, the magnitude of an aerosol mass loss constant is reported to increase with an increase in air motion (turbulence).⁶

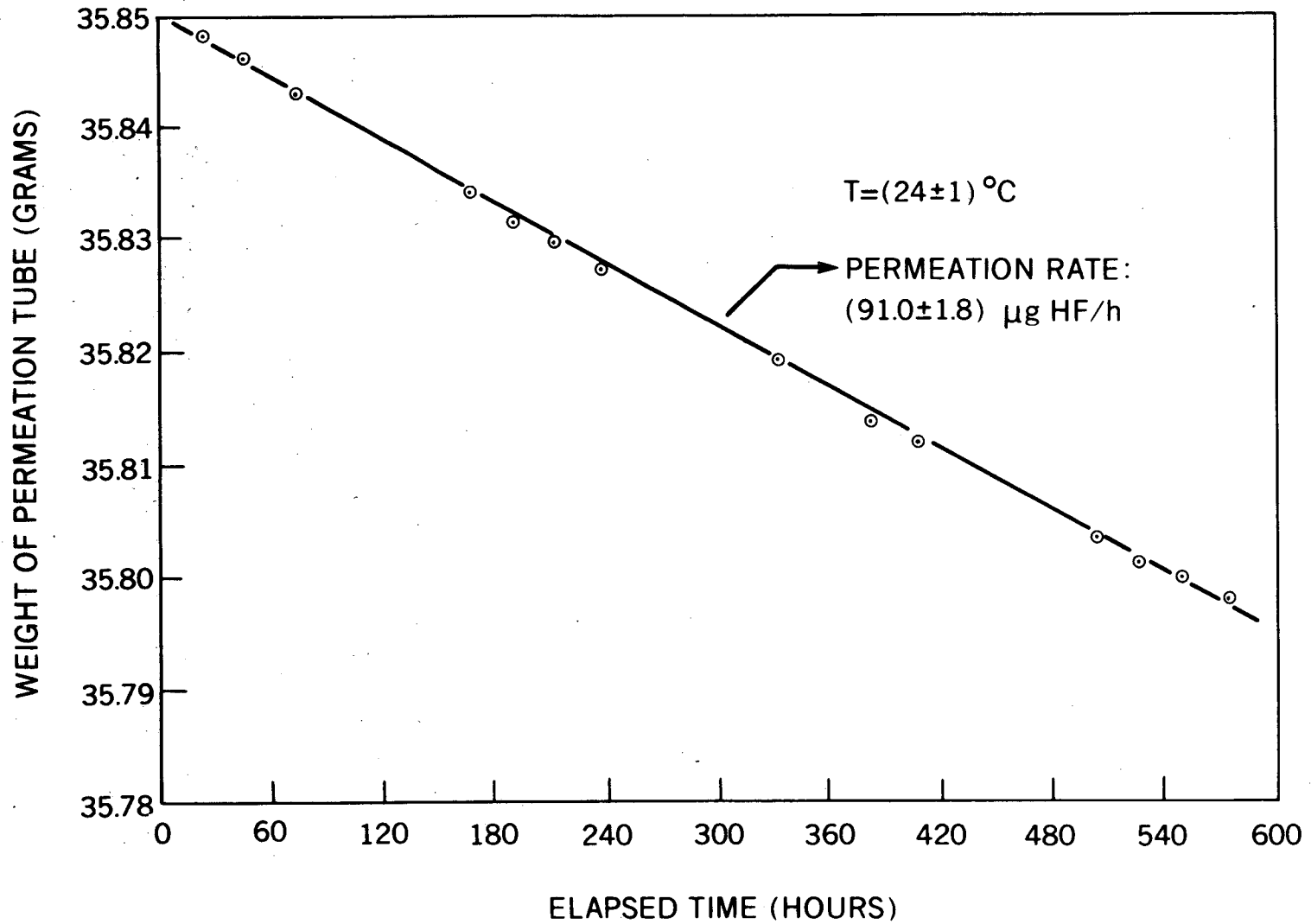


Figure 9. Gravimetric calibration of HF permeation tube.

Table 3. Recovery of HF on membrane filters

Expt. no.	HF mass balance*	Distribution of total recovered HF				
		Prefilter		Treated membrane		Caustic trap HF recovery
		Description	HF recovery	Description	HF Recovery	
1	97.5%	Cellulose acetate, untreated (5µm pore, 25 mm diam)	9.7%	NA	90.2%	
2	98.5%	NA		Cellulose acetate, carbonate-impregnated (0.45 µm pore, 47 mm diam)	99.3%	0.7%
3	99.1%	Teflon (1µm pore 47 mm diam)	<0.003%	Cellulose acetate, formate-impregnated (5 µm pore, 47 mm diam)	97.0%	3.0%

*Total recovered HF, referenced to calibrated permeation rate.

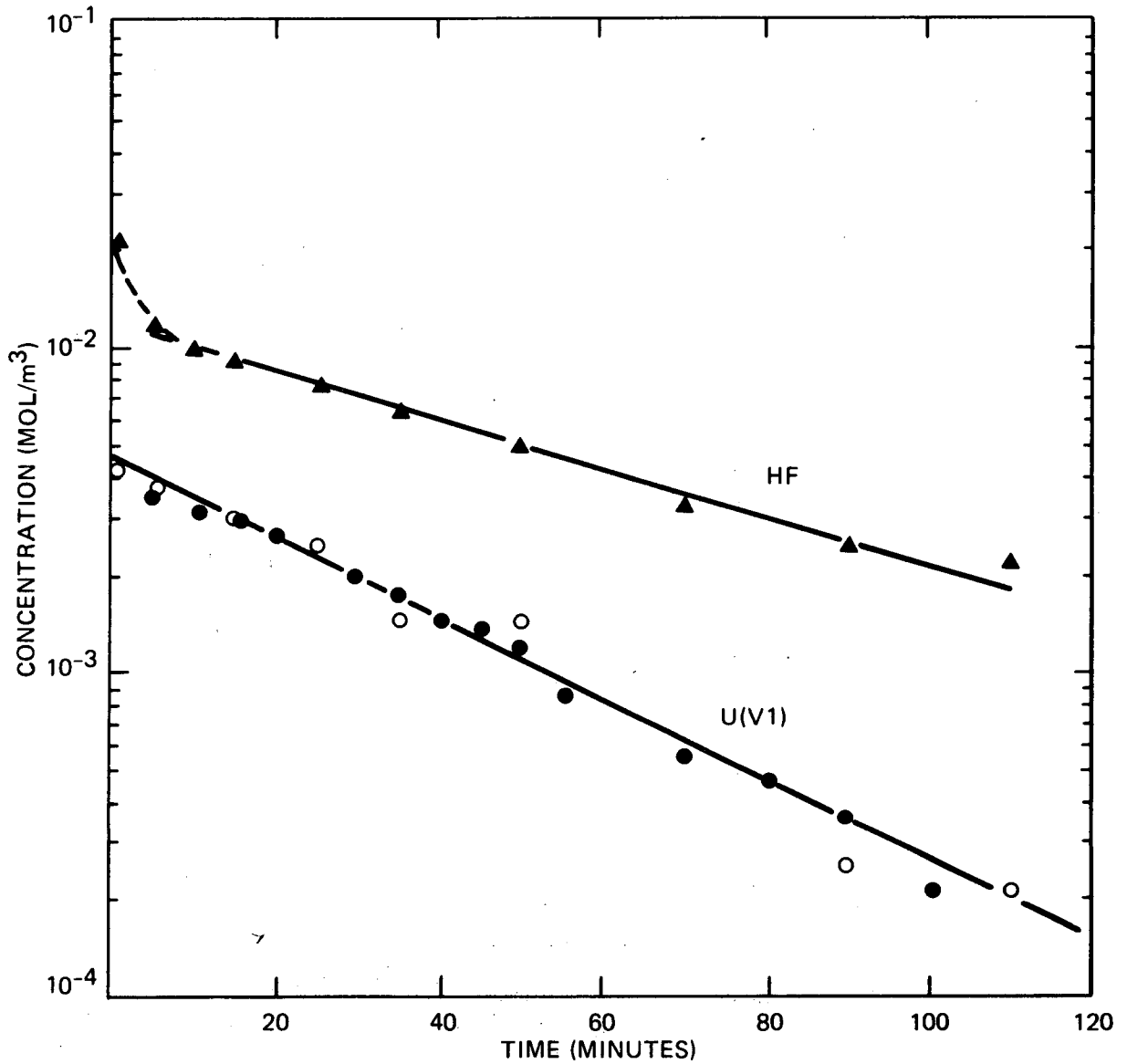


Figure 10. Aerosol measurements following the atmospheric release of UF₆ (~1g in a contained volume of ~0.2 m³). Plotting symbols: (▲), (○) represent results from the chemical analysis of materials collected on membrane filters using a stationary sampling system; (●) represents concentrations of U(VI) as estimated from spectroscopic remote sensing.

REMOTE SENSING OF AEROSOL CONSTITUENTS

Remote sensing of aerosol constituents would be advantageous in providing a real-time, concentration-dependent response to accidental releases of UF_6 . Potentially, remote sensing devices could be employed to determine both the magnitude and the propagation of specific aerosol constituents.

Optical techniques have been applied to the remote measurement of gaseous pollutant concentrations.¹⁸⁻²⁰ Hydrogen fluoride has characteristic absorption in the near-infrared spectral region (Fig. 11), which has been proposed as a basis for selective remote sensing.^{18,21,22} A major difficulty in applying this technique to the detection of HF in the atmosphere is the severe spectral interference due to CO_2 and water vapor--note the poor atmospheric transmission in the region of 2.4 to 2.7 μm as shown in Figure 12. Another potential difficulty is the strong association between HF and H_2O vapor,² which is expected to cause appreciable spectral shifts.

Light scatter is an obvious candidate for the remote sensing of particulate and condensate in aerosol suspensions. Parameters which affect the intensity of the observed light scatter include the following: (1) the intensity of the incident radiation; (2) the angle of observation (relative to the incident beam); (3) the wavelength of the incident radiation; and (4) the quantity, size, shape, and optical properties of the particles.

The geometric dimensions of the UO_2F_2 particulates are comparable in magnitude to the wavelength of visible radiation (0.4 to 0.7 μm); under these circumstances, the scattered radiation is best described as Mie-type scattering, which is strongly concentrated in the forward direction (Mie scatter)--see Figure 13. Due to the complexities of the Mie light-scattering formulae, it is difficult to compute the exact relationship between light scatter and the concentration of a specific particulate aerosol component; however, the transmission of visible light is a valuable, nonintrusive means to monitor the relative settling rate of the aerosol.^{3,5}

The change in forward light transmission, computed as absorbance, is shown in Figure 14B for an experimental release of UF_6 ; this is the identical release for which the chemical data described in Figure 10 were obtained. Note the perturbation in light-scatter signal that occurs when a small volume of gas (e.g. 1% to 5% of total) is sampled (concurrent use of stationary sampling system) and is returned to the experimental chamber, temporarily introducing a small amount of turbulence.

Comparison of the light scatter (Fig. 14B) to the chemical analyses (Fig. 14A) indicates that light scatter is indeed a sensitive means for the detection of aerosol. However, the technique is inherently non-specific. Techniques related to light scatter, but which can provide specific chemical information, include fluorescence and Raman spectroscopy.

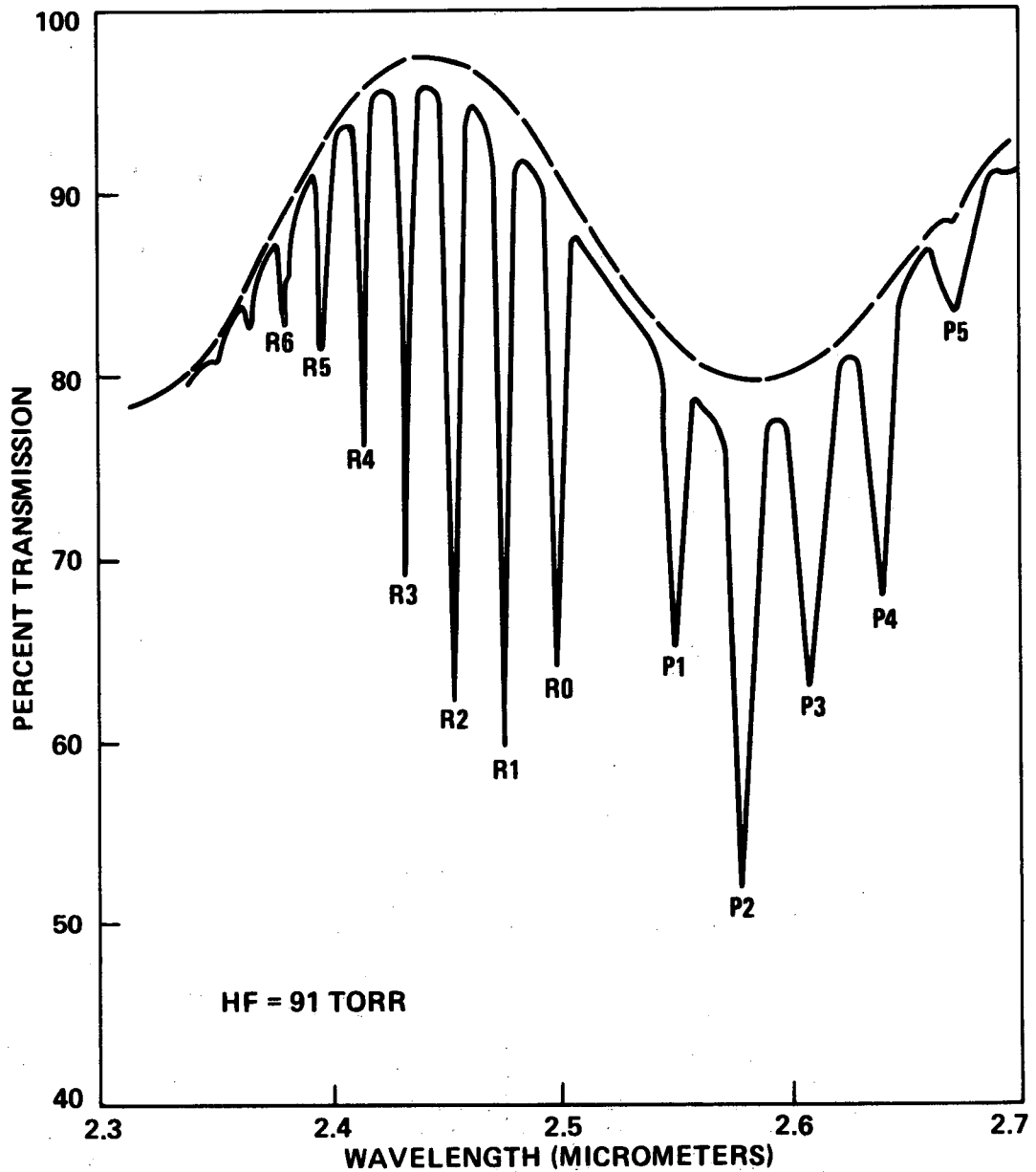
DWG. NO. K/G-84-611
(U)

Figure 11. Absorption spectrum of HF vapor (dashed line represents measurement cell blank).

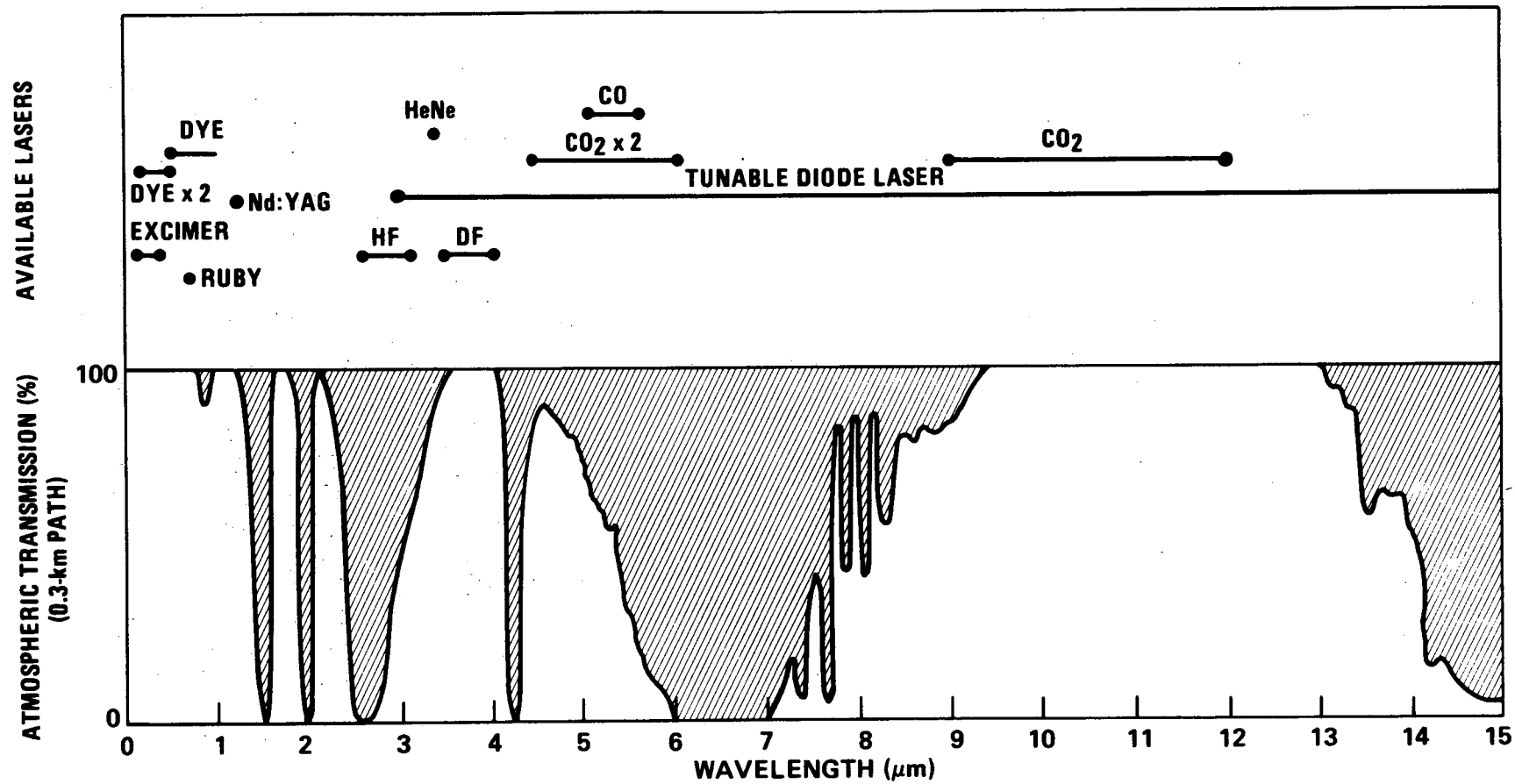


Figure 12. Top: Wavelengths for emission by selected laser systems. Bottom: Atmospheric transmission (0.3-km path), as a function of wavelength. Source: Air Pollution Control Assoc.

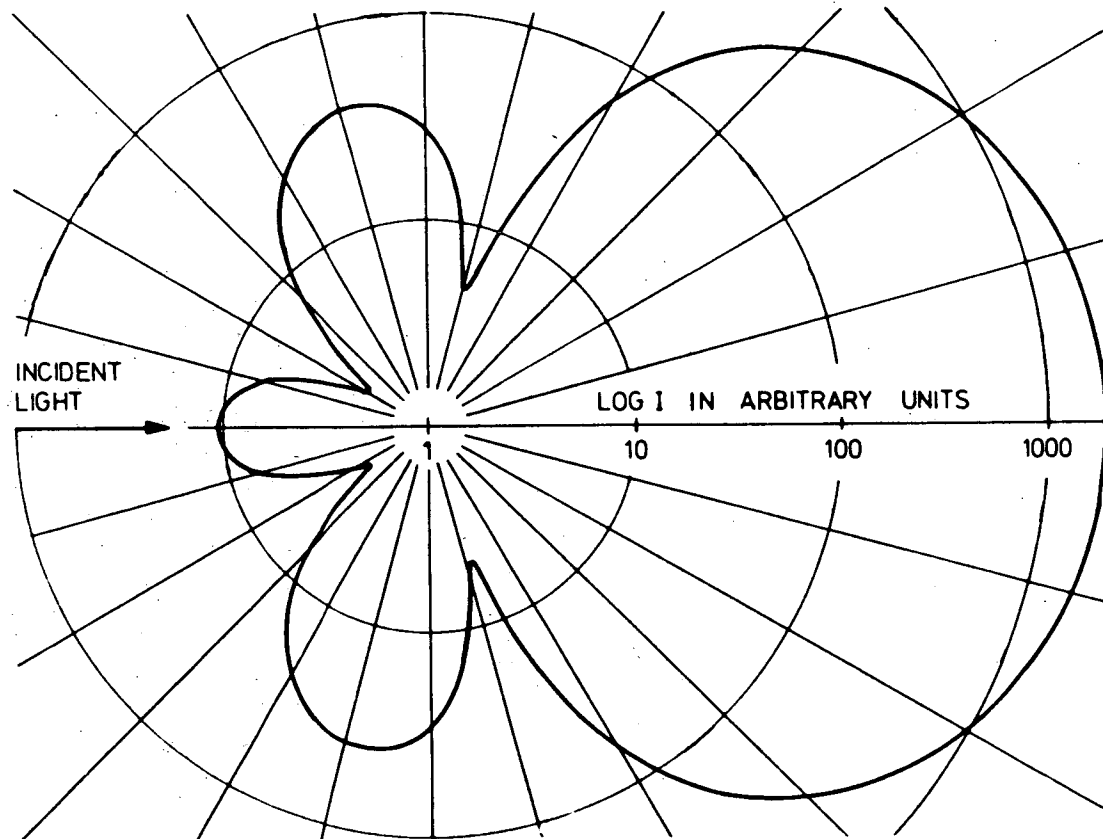


Figure 13. Scattering intensities of a sphere with diameter equal to the wavelength of the light, index of refraction 1.35.
Source: H. Malissa (ed.) Analysis of airborne particulates by physical methods, CRC Press, Inc. (1978),
p. 13. With permission.

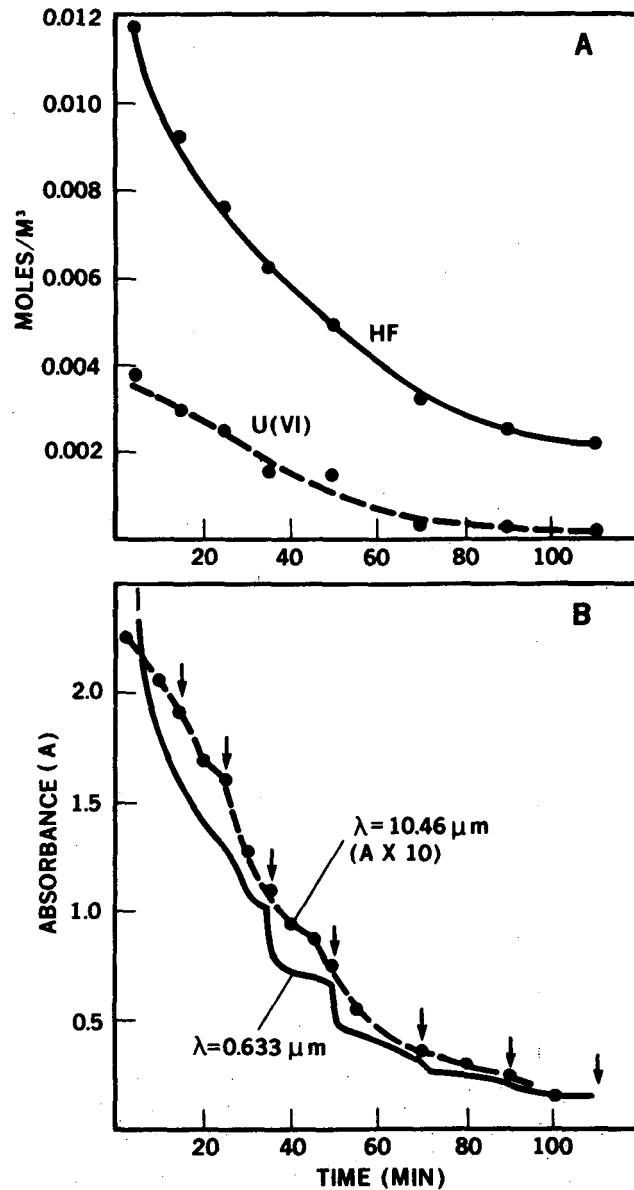


Figure 14. Aerosol measurement following the atmospheric release of UF_6 (~ 1 g in a contained volume of ~ 0.2 m³). (A) Results from the chemical analysis of materials collected on membrane filters using an isokinetic sampling system. Particulate UO_2F_2 is collected on a 1- μm pore Teflon prefilter, and HF is chemisorbed on a formate-impregnated cellulose acetate membrane. (B) Absorbance measurements (~ 60 cm pathlength), as performed with use of (1) a HeNe laser (solid line; $\lambda = 0.633 \mu\text{m}$), representing Mie scatter, and (2) a CO₂ laser (broken line; $\lambda = 10.46 \mu\text{m}$), representing uranyl ion concentration. CsI windows were inserted into the test chamber to permit transmission of the IR radiation. Arrows indicate times at which samples were withdrawn for chemical analysis (see Figure 14A)

Many uranyl salts are fluorescent. In solution phase, fluoride ion strongly enhances fluorescence intensity,²³ as shown in Figure 15. However, we noted very little fluorescence response for uranyl fluoride in the solid phase (e.g., as little as 0.3% of the response measured for uranyl nitrate)--see Table 4. The fluorescence of solid-phase uranyl salts appear to be strongly affected by crystal properties and by the extent of hydration.²⁴

A sample of $\alpha\text{-UO}_2\text{F}_2 \cdot 1.5\text{H}_2\text{O}$, with relatively large crystals, produced an intense Raman signal at 868 cm^{-1} , attributable to the symmetric stretching frequency of the uranyl ion. Unfortunately, the very small particles from UF_6 -release fallout failed to give a signal which was distinguishable from background; presumably, this is due to the extensive rescatter of the weak Raman signal stimulated with $0.514\mu\text{m}$ radiation.

Particulate material from the plume produced in an experimental release of UF_6 was collected onto a hydrophobic polyvinylchloride membrane filter using the previously described sampling device. The exposed membrane was then scanned directly in an infrared (IR) spectrometer. (A similar procedure has been used for the direct IR analysis of free crystalline silica in respirable dust.²⁵) The spectra of this sample and of an unexposed membrane are shown in Figure 16. A strong sample-specific absorption is evidenced at $\sim 955\text{ cm}^{-1}$ ($\sim 10.5\mu\text{m}$), due to the asymmetric stretching frequency of the uranyl ion. Additional absorptions are observed at $\sim 1625\text{ cm}^{-1}$ (attributed to waters of hydration) and at $\sim 430\text{ cm}^{-1}$ (tentatively attributed to a U-F stretch).

The uranium-selective absorption at $\sim 10.5\mu\text{m}$ offers a convenient means for the remote sensing of UO_2F_2 aerosol. This wavelength is in a region of minimal spectral interference by atmospheric gases and is selectable as the 10P6 transition of a CO_2 laser ($\lambda = 10.46\mu\text{m}$); see Figure 12. An additional advantage is the fact that this wavelength is relatively long compared to the average particle size, thus minimizing scattering effects.

Absorption of radiation at this wavelength during an experimental release of UF_6 is illustrated in Figure 14B. The U(VI)-selective absorption is seen to parallel the nonspecific Mie scatter, but the sensitivity is reduced by an order of magnitude. Also, as expected, the IR absorption closely parallels the U(VI) concentration in the aerosol (Fig. 14A). The combination of chemical and spectral data permit the computation of an absorbance cross section (σ):

$$\sigma = \frac{2.303 A}{n l} \quad (4)$$

where A = Absorbance

n = Molecules/ cm^3

l = Absorption pathlength, cm.

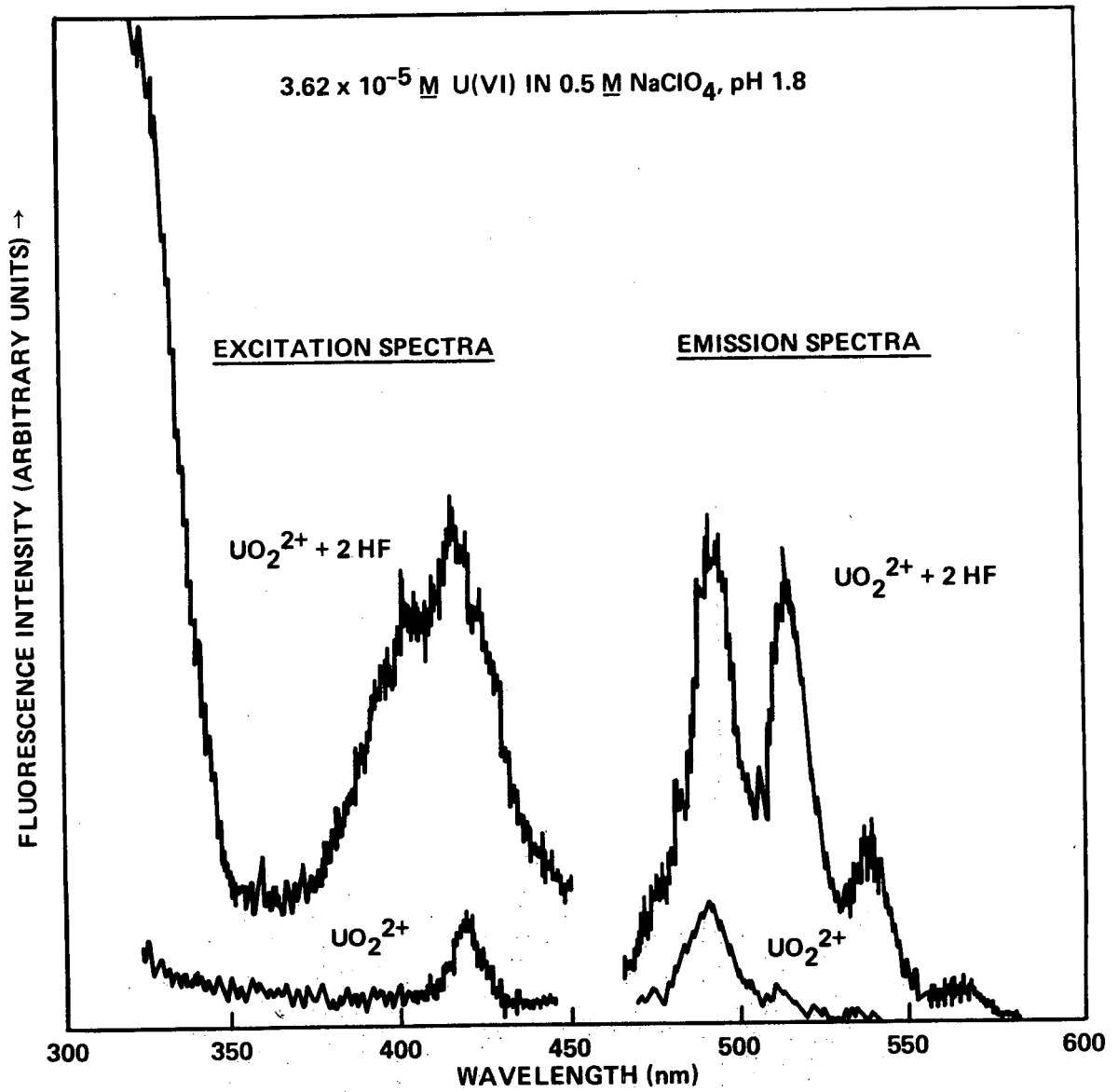


Figure 15. Fluorescence excitation and emission spectra for uranyl ion in solution phase.

Table 4. Solid-phase fluorescence

Sample	Intensity (arbitrary units)
Background	0.1
$\text{UO}_2\text{F}_2 \cdot 1.5 \text{H}_2\text{O}$	19.2
" UO_2F_2 " (Recent aerosol deposition products)	1.8
$\text{UO}_2(\text{C}_2\text{H}_3\text{O}_2)_2 \cdot 2\text{H}_2\text{O}$	420.0
$\text{UO}_2(\text{NO}_3)_2 \cdot 6\text{H}_2\text{O}$	585.0

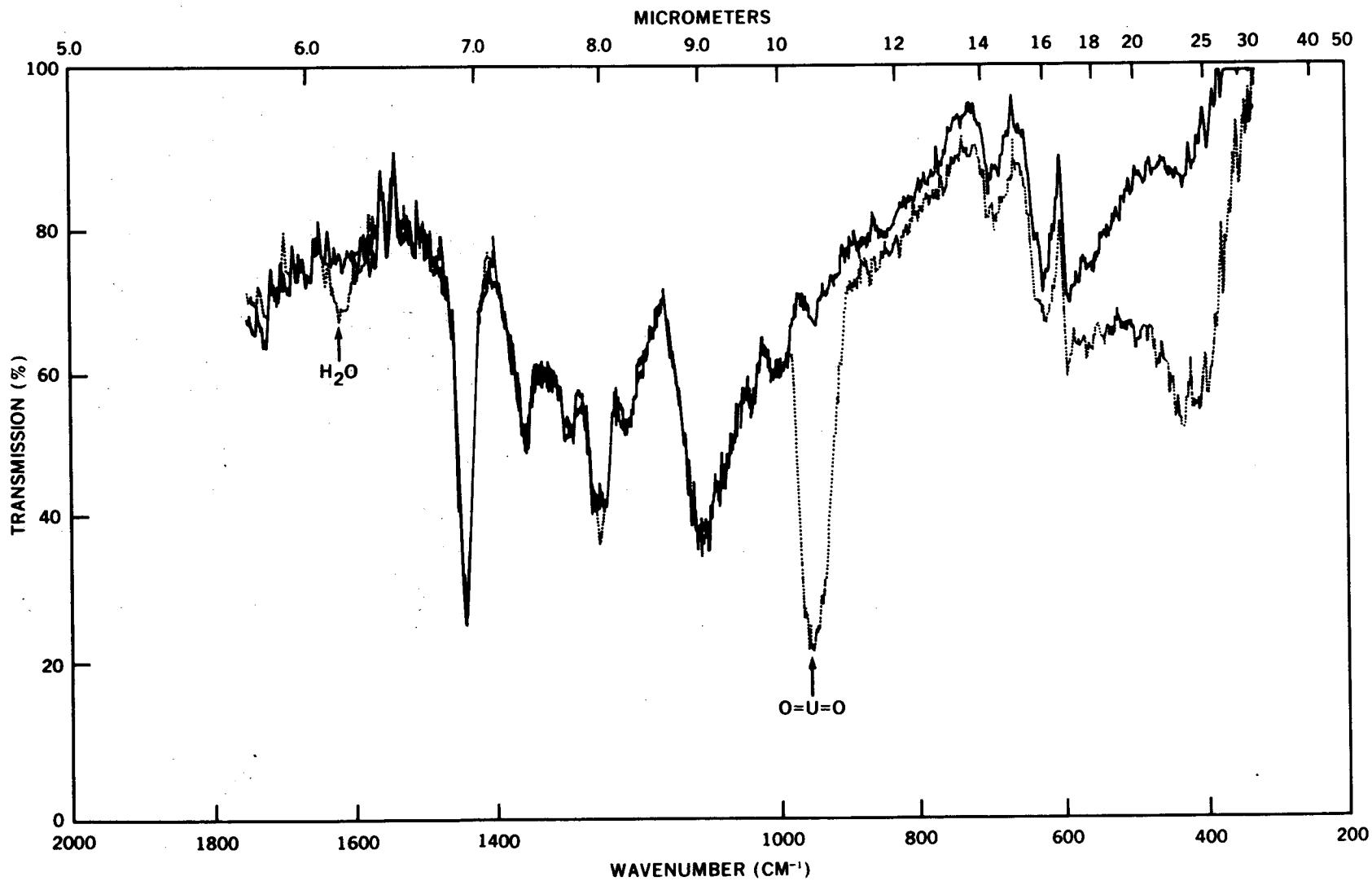


Figure 16. Direct infrared spectrum of $\text{UO}_2\text{F}_2 \cdot n \text{H}_2\text{O}$ aerosol (broken line), as collected on a PVC membrane filter (solid line).

The absorbance cross section estimated for UF_6 , UO_2F_2 , and HF at their IR absorption maxima are compared in Table 5; note that the sensitivity for UO_2F_2 [as U(VI)] is approximately two orders of magnitude greater than that for HF.

CONCLUSION

In conclusion, we have used a variety of physical and chemical techniques to examine the products from the atmospheric hydrolysis of UF_6 . Of all the properties of the aerosol, the most salient is the small size of the UO_2F_2 particles which are produced. Particle size affects the mode of dispersion and the rate of sedimentation of these particulates. The particles are formed in the size range of "respirable dust," thus affecting the mode and extent of their ingestion (and, hence, their toxicological effect).

Particle size also affects the efficiency for the collection of aerosol with the use of stationary sampling devices and the sensitivity for the remote sensing of the materials with use of such nonselective physical measurements as ionized smoke detection or light scatter.

In the text, we describe an improved sampling procedure for the separate collection of particulate fluorides and HF vapor. With the use of this technique, we are able to compute the sedimentation rates for each component of the aerosol and to demonstrate the more rapid sedimentation of the uranyl fluoride component.

We demonstrate the applicability of laser spectroscopy (Mie scatter and IR absorbance measurements) for the remote sensing of aerosol components. The uranyl-selective absorbance at $\sim 10.5\mu m$ is recommended for the quantitative remote measurement of the concentration of the uranium component of the aerosol.

Table 5. Absorption cross sections (σ) for selected compounds at their IR absorption maxima

Compound	λ (μm)	σ (cm^2)
Uranium hexafluoride	16.00	6×10^{-18}
Uranyl fluoride	10.46	4×10^{-18}
Hydrogen fluoride	2.45	6×10^{-20}

REFERENCES

1. L. H. Brooks, E. V. Garner, and E. Whitehead, IGR-TN/CA 277, Chemical and X-ray Crystallographic Studies of Uranyl Fluoride, United Kingdom Atomic Energy Authority, Capenhurst, Ches., England, February 1956.
2. W. H. McCulla, Determination of the Rate of HF Hydration and the Effects of HF on Moisture Condensation, K/PS-155, Union Carbide Corp. Nuclear Div., Oak Ridge Gaseous Diffusion Plant, April 1982.
3. P. W. Pickrell, Characterization of the Solid, Airborne Materials Created by the Interaction of UF₆ with Atmospheric Moisture in a Contained Volume, K/PS-144, Union Carbide Corp. Nuclear Div., Oak Ridge Gaseous Diffusion Plant, April 1982.
4. A. A. Tsvetkov, V. P. Seleznev, B. N. Sudarikov, and B. V. Gromov, "Equilibrium Diagram of the Uranyl Fluoride-Water System," Russian J. Inorg. Chem., 17, 1048 (1972).
5. C. J. Lux, Evaluation of Techniques for Controlling UF₆ Release Clouds in the GAT Environmental Chamber, GAT-T-3116, Goodyear Atomic Corporation, Piketon, Ohio, April 1982.
6. H. L. Green and W. R. Lane, Particulate Clouds: Dusts, Smokes and Mists (2nd ed.), D. Van Nostrand Co., Inc., Princeton (1964), p 67 ff.
7. C. K. Bayne, Personal Communication, Oak Ridge National Laboratory, March 1984.
8. J. Ishida, G. Sakamoto, S. Takeda, and J. Kato, PNCT 831-79-02, Investigation of the UF₆ Aerosol Behavior in Air, IV, The Characteristics of Monitors Detecting UF₆ Release, Tokai Works Semi-Annu. Rep. 1978 (pub. 1979).
9. R. Maurodineau and R. R. Coe, "Improved Apparatus and Procedures for Sampling and Analyzing Air for Fluorides," Contrib. Boyce Thompson Inst., 18, 173 (April-June 1955).
10. "Analytical Guide: Inorganic Fluorides," Amer. Ind. Hygiene J., 36, 701 (1975).
11. C. R. Thompson, et al, "Analytical Method for Fluorides and Hydrogen Fluoride in Air," Health Lab. Sci., 12, 242 (1975).
12. L. A. Elfers and C. E. Decker, "Determination of Fluoride in Air and Stack Gas Samples by Use of an Ion Specific Electrode," Anal. Chem., 40, 1658 (1968).
13. T. Okita, K. Kaneda, T. Yanaka, and R. Sugar, "Determination of Gaseous and Particulate Chloride and Fluoride in the Atmosphere," Atmos. Environ., 8, 927 (1974).

14. "Ambient Air Sampling for Fluoride, Uranium, and Chromium-Filter Method," Environmental Analysis Procedure Manual, Union Carbide Corp. Nuclear Div., Procedure No. EC-1544, March 1979.

15. "Uranium (Total) in Water, Fluorometric Method," Environmental Analysis Procedure Manual, Union Carbide Corp. Nuclear Div., Procedure No. EC-191, February 1979.

16. F. P. Scaringelli, A. E. O'Keefe, E. Rosenburg, and J. P. Bell, "Preparation of Known Concentrations of Gases and Vapors with Permeation Devices Calibrated Gravimetrically," Anal. Chem., 42, 871 (1970).

17. G. L. Grametbauer, "A Portable, Programmable, Remotely Operated Air Sampler System," Presented at the 1983 UCC-ND and GAT Environmental Protection Seminar, Oak Ridge Gaseous Diffusion Plant, December 7, 1983.

18. W. F. Hergret and J. D. Brasher, "Remote Measurement of Gaseous Pollutant Concentrations Using a Mobile Fourier Transform Interferometer System," Appl. Optics, 18, 3404 (1979).

19. G. E. Schweitzer, "Airborne Remote Sensing," Environ. Sci. Tech., 16, 6 (1982).

20. H. L. Schiff, D. R. Hastie, G. L. Mackay, T. Iguchi, and B. A. Ridley, "Tunable Diode Laser Systems for Measuring Trace Gases in Tropospheric Air," Environ. Sci. Tech., 17, 352A (1983).

21. Anonymous, "He-Ne Lasers in Pollutant Control," Laser Focus/Electro-Optics, November 1983, p. 34.

22. Anonymous, "Hydrogen Fluoride Monitor," Application note from Spectra-Physics Laser Analytics Division, Bedford, MA, 1983.

23. M. Moriyasu, Y. Yokoyama, and S. Ikeda, "Anion Coordination to Uranyl Ion and the Luminescence Lifetime of the Uranyl Complex," J. Inorg. Nucl. Chem., 38, 1329 (1976).

24. F. Rabinowitch and R. L. Belford, Spectroscopy and Photochemistry of Uranyl Compounds, Oxford, 1964, pp. 55-56.

25. D. Toffolo and J. N. Lockington, "Direct Infrared Spectrophotometric Analysis of Free Crystalline Silica in Respirable Dust from a Steel Foundry," Am. Indust. Hygiene Assoc. J., 42, 579 (1981).